ELSEVIER

Nuclear Instruments and Methods in Physics Research A 463 (2001) 42–49

NUCLEAR INSTRUMENTS & METHODS IN PHYSICS RESEARCH Section A

www.elsevier.nl/locate/nima

Development of a traveling wave resonant ring of the JNC high-power, high-duty electron linac

Masahiro Nomura[a,*], Y.L. Wang[a], Yoshio Yamazaki[a], Koichiro Hirano[a], Yuko Kato[b], Takehiro Ishikawa[c], Tomoki Komata[c], Toru Hiyama[c]

[a] *System Engineering Division, Oarai Engineering Center, Japan Nuclear Cycle Development Institute, 4002 Narita-cho, Oarai-machi, Ibaraki-ken 311-1393, Japan*

[b] *NESI, 4002 Narita-cho, Oarai-machi, Ibaraki-ken 311-1393, Japan*

[c] *PESCO, 4002 Narita-cho, Oarai-machi, Ibaraki-ken 311-1393, Japan*

Received 20 June 2000; received in revised form 3 November 2000; accepted 5 November 2000

Abstract

We present experimental results for a traveling wave resonant ring in a low-duty beam test and a high-duty RF test. In the low-duty beam test, we studied the RF characteristics of the traveling wave resonant ring and measured the multiplication factor, M, and conversion efficiency, η. We obtained multiplication factors of 3.2 under no beam loading and 2.2 under a beam loading of 100 mA and these were in good agreement with calculations. A high conversion efficiency of 0.74 was achieved by using the traveling wave resonant ring. In the high-duty RF test, we measured the multiplication factor as a function of phase shifter position and temperature of the traveling wave resonant ring. From the experimental results, we calculated the variation of the phase shifter position to a temperature rise. Understanding this variation is necessary to keep the multiplication factor at the maximum for the design point 20% duty operation.

PACS: 29.17

Keywords: Traveling wave resonant ring; High-power; High-duty electron linac

1. Introduction

The Japan nuclear cycle development institute (JNC) is developing a high-power, high-duty electron linac to study the feasibility of nuclear waste transmutation [1]. In order to achieve transmutation with accelerators, it is necessary to increase the average beam current and improve efficiency. In order to increase the threshold current level of the beam break-up, we adopted 1249.135 MHz (L-Band) as the accelerating frequency of the JNC linac. To improve the efficiency of the JNC linac, we used a traveling wave resonant ring (TWRR) [2,3]. The main specifications and a schematic layout of the JNC linac are given in Table 1 and Fig. 1, respectively.

Construction of the JNC linac was started in 1989. The facility was completed in 1996 and the first beam commissioning was started in 1998. By

*Corresponding author. Fax: +81-29-267-5180.
E-mail address: nomura@oec.jnc.go.jp (M. Nomura).

0168-9002/01/$ - see front matter
PII: S0168-9002(01)00229-7

December 1999, an electron beam with a macropulse average beam current of 100 mA, a pulse width of 1 ms and a repetition of 35 pps was accelerated up to 7 MeV.

The TWRR consists of a traveling wave accelerator guide [4], a waveguide, a main directional coupler, a dummy load, two directional couplers to measure the forward and backward power in the TWRR, three stub tuners and a phase shifter. A general view of the TWRR is shown in Fig. 2. The accelerator guide is designed to have a constant gradient structure under a beam loading of 100 mA and employs thirteen $2\pi/3$ mode cavities and two coupling cavities. The coupling of the main directional coupler is designed to be optimized under a beam loading of 100 mA. The three stub tuners are to cancel the reflection in the TWRR for proper matching. The phase shifter consists of three stub tuners. These tuners are set at the same position and move together. The phase shifter is to adjust the phase length of the TWRR in order to maintain the resonance frequency when the phase length is changed due to fluctuations in temperature. The three stub tuners and the phase shifter serve to obtain the maximum value of the multiplication factor because the TWRR achieves the maximum value at resonance and with no reflection.

First, we studied the RF characteristics of the TWRR and measured the multiplication factor and conversion efficiency for a low-duty beam test. Next, we measured the multiplication factor as a function of phase shifter position and temperature of the TWRR in a high-duty RF test.

Table 1
Main specifications of the JNC linac

Accelerating frequency f	1249.135 MHz
Repetition R	50 pps
Pulse width W	4 ms
Duty D	20%
Macropulse average beam current I_b	100 mA
Average beam current I_{av}	20 mA
Beam energy E	10 MeV
Number of accelerator guides	8
Number of klystrons	2
RF power of klystron	1.2 MW (CW)

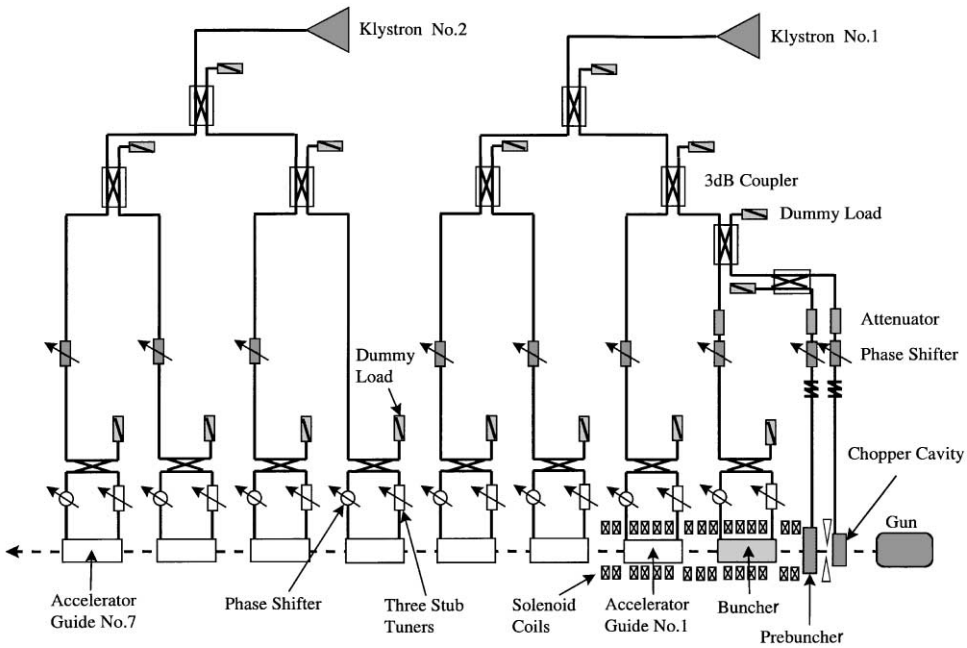

Fig. 1. Schematic layout of the JNC linac.

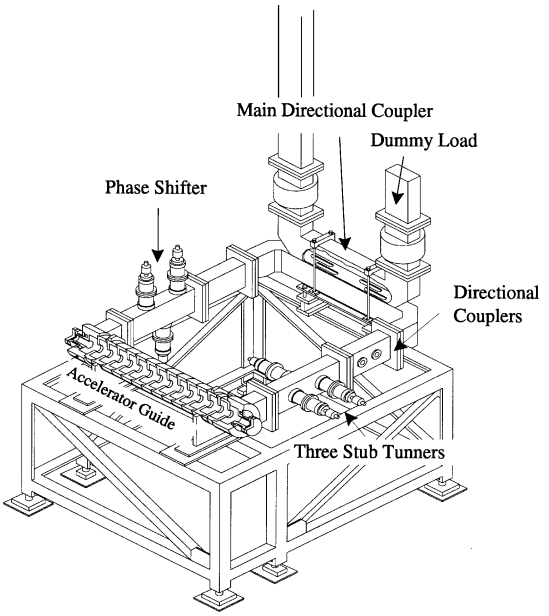

Fig. 2. General view of the TWRR. The TWRR consists of a traveling wave accelerator guide, a waveguide, a main directional coupler, a dummy load, two directional couplers, three stub tuners and a phase shifter.

2. Low-duty beam test

The purposes of the low-duty beam test were to study the RF characteristics of the TWRR and measure the multiplication factor and conversion efficiency by means of an electron beam with a macropulse average current of 100 mA. In this test, we lowered the duty to remove temperature instability. The experimental conditions are shown in Table 2.

We measured the forward power P_F and backward power P_B in the TWRR with the first accelerator guide and the power to the dummy load P_D. The experimental results and specifications of the TWRR with the first accelerator guide are shown in Fig. 3 and Table 3, respectively. As seen in Fig. 3, the backward power P_B is small compared to the input power P_0. This means that the reflection in the TWRR is nearly canceled by adjusting the three stub tuners. Further, Fig. 3 shows that little power goes into the dummy load under a beam loading of 100 mA. This means that the TWRR can be made to resonate by adjusting

Table 2
Experimental conditions at the low-duty beam test

Repetition rate R	1 pps
Input macropulse average power P_0	198 kW
RF pulse width W_{RF}	3 ms
Macropulse average beam current I_b	100 mA
Beam width W_b	2 ms
Duty D	0.2%

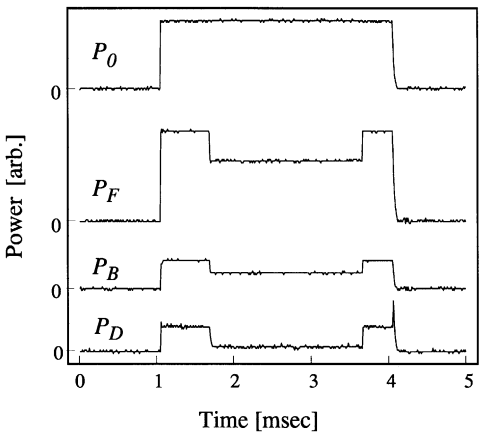

Fig. 3. Powers in the TWRR with the first accelerator guide. The input macropulse average power P_0 is 198 kW. The forward power P_F is 2070 kW under no beam loading and 934 kW under a beam loading of 100 mA. The backward power P_B is 16.3 kW under no beam loading and 5.47 kW under a beam loading of 100 mA. The macropulse average power to the dummy load P_D is 59.2 kW under no beam loading and 2.74 kW under a beam loading of 100 mA. Both the backward power P_B and power to the dummy load P_D can be lowered by adjusting the three stub tuners and the phase shifter.

Table 3
Specifications of the TWRR with the first accelerator guide

Accelerator guide	
Length	1.2 m
Mode	$2\pi/3$
Structure	Constant gradient structure under a beam loading of 100 mA
Number of cavities	15
Periodic length d	8 cm
Attenuation constant	0.0331 Neper
Waveguide	
Attenuation constant	0.0088 Neper
Main directional coupler	
Coupling coefficient C	0.4479
Directivity	−32.03 db
Voltage transmission coefficient T_r	0.959

the phase shifter. The TWRR has good RF characteristics.

The multiplication factor M of the TWRR can be calculated from the experimental results of P_0 and P_F by means of Eq. (1) [5]

$$M = \sqrt{\frac{P_F}{P_0}} \tag{1}$$

where $M = 3.2$ under no beam loading, $M = 2.2$ under a beam loading of 100 mA.

The multiplication factor M can also be calculated theoretically using the following procedure. Starting with the input power P_0 that passes through the main directional coupler into the TWRR, the forward power P_F is

$$P_F = C^2 P_0 \tag{2}$$

where C is the coupling coefficient of the main directional coupler. The forward power P_F passes into the first cavity of the accelerator guide through the waveguide. The electric field $E_1(z)$ at a position z in the first cavity can be calculated by means of the attenuation coefficient, α_1, shunt impedance of the first cavity, r_1, periodic length, d, and beam current, I_b

$$E_1(z) = \sqrt{2\alpha_1 r_1 P_F} e^{-\alpha_1 z} - I_b r_1 (1 - e^{-\alpha_1 z}). \tag{3}$$

The power P_1 that has passed through the first cavity is:

$$P_1 = P_F e^{-2\alpha_1 d} - I_b \int_0^d E_1(z)\, dz. \tag{4}$$

In a similar manner, the power P_{15} that has passed through the last cavity can be calculated. The power P_{15} transits the main directional coupler and adds to the forward power P_F. The forward power P_F passes into the first cavity again. In this way, the forward power P_F is enhanced until the input power P_0 is in equilibrium with the power loss in the TWRR. From the foregoing equations, the multiplication factor M can be calculated theoretically

$M = 3.15$ under no beam loading

$M = 2.03$ under a beam loading of 100 mA.

The experimental results are in good agreement with these calculations.

The conversion efficiency η of the TWRR is defined as the fraction of the input power P_0 that is converted to the beam power P_{Beam}

$$\eta = \frac{P_{Beam}}{P_0}. \tag{5}$$

From the forward power P_F in Fig. 3 and Eqs. (3), (4) and (6), the beam power P_{Beam} can be calculated

$$P_{Beam} = I_b \sum_{n=1}^{15} \int_0^d E_n(z)\, dz \tag{6}$$

where $E_n(z)$ is the electric field at a position z in the nth cavity. The conversion efficiency η is

$\eta = 0.74$.

In the case of a simple traveling wave accelerator guide, η can be calculated for the forward power $P_F = P_0$ in Eqs. (3) and (4)

$\eta = 0.32$.

It is clear that a high conversion efficiency of 0.74 was achieved by using the TWRR.

3. High-duty RF test

The purpose of the high-duty RF test was to find out how to keep the multiplication factor maximum by adjusting the phase shifter when the temperature of the TWRR rises in the design point 20% duty operation. At the design point 20% duty operation, 40 kW of RF power is fed into the TWRR. A portion of this power, 28 kW, is used for beam acceleration, and the remainder, 12 kW, is dissipated in the TWRR, raising its temperature. The cooling system supplies the TWRR with cooling water at a temperature of $30 \pm 0.1^{\circ}C$. The cooling system cannot keep the temperature of the TWRR constant in this high-duty operation. The temperature rise is estimated to be $3^{\circ}C$ in the 20% duty operation. The decrease in multiplication factor due to the temperature rise must be controlled with the phase shifter.

To find the variation of the phase shifter position to a temperature rise, we measured the multiplication factor of the TWRR with the first accelerator guide as a function of phase shifter

Table 4
Experimental conditions (phase shifter position dependence)

Temperature T	28.3°C
Phase shifter position x	0.6–9.6 mm
Input macropulse average power P_0	193 kW
Repetition R	1 pps
RF pulse width W_{RF}	1.6 ms

Table 5
Experimental conditions (temperature dependence)

Temperature T	28.3–31.7°C
Phase shifter position x	8.6 mm
Input macropulse average power P_0	193 kW
Repetition R	1–35 pps
RF pulse width W_{RF}	1.6–4.0 ms

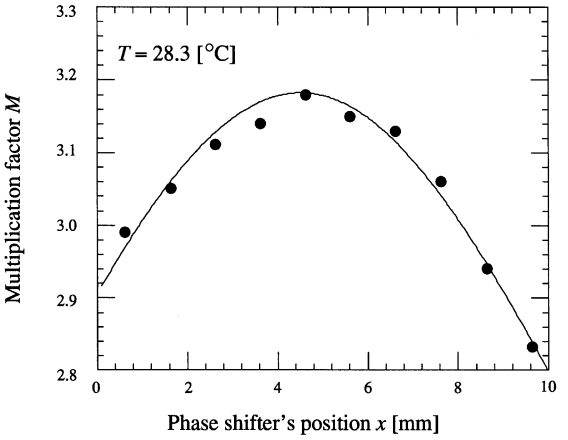

Fig. 4. The phase shifter position dependence of the multiplication factor M. The phase shifter changes the phase length of the TWRR, and consequently, the multiplication factor M changes. The multiplication factor M has the maximum value at the resonance. Data are fitted by Eq. (8).

position and temperature. In this high-duty RF test, we did not accelerate an electron beam because in a high-duty operation test like this the accelerator guides and beam ducts are at risks of being damaged by the electron beam whose trajectory is affected by a fluctuation of the power in the TWRR.

First, we measured how M depends on the phase shifter position. The experimental conditions and results are shown in Table 4 and Fig. 4, respectively. Fig. 4 shows that the phase shifter changes the phase length of the TWRR, and consequently, the multiplication factor changes. The multiplication factor is maximum at resonance. Next, we measured the temperature dependence of M. The temperature of the TWRR was changed from 28.3°C to 31.7°C with the RF pulse width W_{RF} and repetition rate R. The temperature was measured with three thermocouples installed in the upstream, midstream and downstream portion of the accelerator guide. The average of the three was taken as the temperature of the TWRR. The experimental conditions and results are shown in Table 5 and Fig. 5, respectively. Fig. 5 shows that as the phase length of the TWRR changes with temperature, so also the multiplication factor changes with the temperature.

If we assume that there is no reflection in the TWRR and that the main directional coupler is ideal one with infinite directivity, the multiplication factor M of the TWRR can be written [3]

$$M = \frac{C}{\sqrt{1 + T_r^2(1 - C^2) - 2T_r\sqrt{1 - C^2}\cos\phi}} \tag{7}$$

where T_r and ϕ are the voltage transmission coefficient and phase length of the TWRR. If the TWRR is at resonance, the phase length $\phi = 2n\pi$ ($n = 1, 2, 3, \ldots$) and the multiplication factor is a maximum. The phase length ϕ depends on the temperature of the TWRR and can be adjusted with the phase shifter. To find the dependence of phase length on phase shifter position, $\Delta\phi/\Delta x$, and temperature, $\Delta\phi/\Delta T$, we make Eq. (8) fit both the experimental results as shown in Figs. 4 and 5

$$M = a + \frac{C}{\sqrt{1 + T_r^2(1 - C^2) - 2T_r\sqrt{1 - C^2}\cos\{\Delta\phi/\Delta x(x - x_0) + \Delta\phi/\Delta T(T - T_0)\}}} \tag{8}$$

where x_0 is the phase shifter position at the resonance at the temperature T_0 that is the temperature of the TWRR in low-duty operation. The parameter a is the fitting parameter that

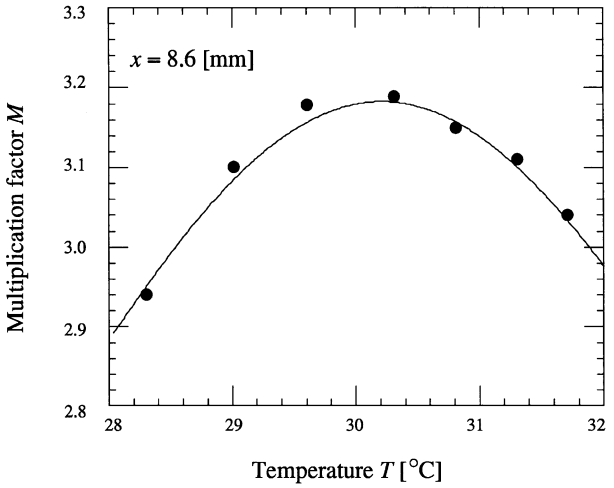

Fig. 5. Temperature dependence of the multiplication factor M. The temperature of the TWRR is measured by three thermocouples that are installed in the upstream, midstream and downstream portion of the accelerator guide. The average of these three temperatures is adopted for the temperature. Since the phase length of the TWRR changes with temperature, the multiplication factor M also changes with temperature. Data are fitted by Eq. (8).

includes experimental error. The results of the fitting are shown with solid lines in Figs. 4 and 5 and the parameters are listed in Table 6.

First, we compare the experimental result of $\Delta\phi/\Delta x$ to an individual phase shifter test result. In the individual test, we measured the ratio $\Delta\phi/\Delta x$ as 0.93 deg/mm. The experimentally measured ratio of $\Delta\phi/\Delta x$ of 0.88 deg/mm agrees well with the individual test result.

Next, we discuss the experimental result for $\Delta\phi/\Delta T$. The ratio $\Delta\phi/\Delta T$ can be calculated theoretically

$$\frac{\Delta\phi}{\Delta T} = \frac{2\pi\alpha l_w \lambda_{gw}}{\lambda_0^2} + \frac{2\pi l_a}{\lambda_{ga}} \frac{c}{v_{ga}} \frac{1}{f} \frac{\Delta f}{\Delta(2b)} \alpha(2b) \qquad (9)$$

where l_w and λ_{gw} are the length and the wavelength of the waveguide and l_a and λ_{ga} are the length and the wavelength of the accelerator guide, respectively. The v_{ga} is the group velocity in the accelerator guide, λ_0 is the wavelength in a vacuum, b is the inside diameter of the accelerator guide, f is the accelerating frequency, α is the line expansion coefficient and c is the velocity of light. The first term shows the change of the phase length associated with the waveguide and the second term is the change of the phase length associated with the accelerator guide. The second term is about ten times larger than the first one. From Eq. (9), the ratio $\Delta\phi/\Delta T$ is calculated to be -1.3 deg/°C. The experimentally determined ratio $\Delta\phi/\Delta T$ of -1.9 deg/°C is different from the theoretical calculation. Looking at Eq. (9), the ratio $\Delta\phi/\Delta T$ depends strongly on the inside diameter of the accelerator guide. This means that the ratio $\Delta\phi/\Delta T$ strongly depends on the temperature inside the TWRR. In practice, it is difficult to measure this inside temperature. As mentioned earlier, the cooling water system cannot keep the temperature of the TWRR constant in a high-duty operation as in this test. The cooling system just supplies the TWRR with controlled cooling water, and consequently, temperature gradients occur as the temperature of the TWRR rises. The discrepancy between the experimental result and calculation is most likely caused by the

Table 6
Parameters

a	0.045
x_0	4.5 (mm) (at $T_0 = 28.3$°C)
$\Delta\phi/\Delta x$	0.88 (deg/mm)
$\Delta\phi/\Delta T$	-1.9 (deg/°C)

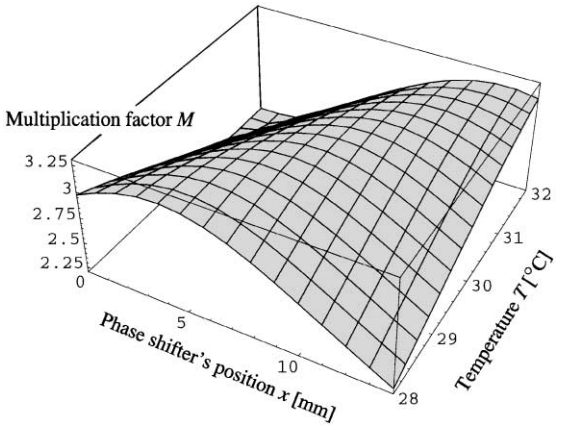

Fig. 6. Graph of the multiplication factor M as a function of phase shifter position x and temperature T. This graph shows that if the temperature of the TWRR rises, the phase shifter must be adjusted so that the multiplication factor M is maintained at the maximum.

temperature gradients between the inside and the measuring points because we measured the ratio $\Delta\phi/\Delta T$ of $-1.2\,\mathrm{deg}/^{\circ}\mathrm{C}$ when the temperature of the whole TWRR was changed from 30°C to 36°C with the cooling water system.

Finally, we calculated the variation of the phase shifter position to the temperature rise of the TWRR from the ratios, $\Delta\phi/\Delta x$ and $\Delta\phi/\Delta T$. The ratio $\Delta x/\Delta T$ is

$$\frac{\Delta x}{\Delta T} = -2.1\ \mathrm{mm}/^{\circ}\mathrm{C} \tag{10}$$

We can keep the multiplication factor maximum by adjusting the phase shifter according to Eq. (10) when the temperature of the TWRR rises in the 20% duty operation. This procedure means that the multiplication factor is kept at the maximum, as shown in Fig. 6, by adjusting the phase shifter in proportion to the temperature rise. The proportional ratio corresponds to the ratio $\Delta x/\Delta T$.

4. Summary

We studied the RF characteristics of the TWRR and measured the multiplication factor M and conversion efficiency η in the low-duty beam test. We measured the forward power P_F and the backward power P_B in the TWRR with the first accelerator guide, along with the power to the dummy load P_D. Both the backward power P_B and power to the dummy load P_D are small compared to the input power P_0. This means that the reflection in the TWRR is canceled by adjusting the three stub tuners and resonance is achieved by adjusting the phase shifter. The TWRR has good RF characteristics. The multiplication factors of 3.2 under no beam loading and 2.2 with a beam loading of 100 mA were obtained and these are in good agreement with the calculations. A high conversion efficiency of 0.74 was achieved by using the TWRR.

In the high-duty RF test, we measured the multiplication factor as a function of the phase shifter position and temperature of the TWRR. First, we calculated the ratios, $\Delta\phi/\Delta x$ and $\Delta\phi/\Delta T$, from the experimental results. The experimental result for $\Delta\phi/\Delta x$ was substantially in agreement with an individual test result on the phase shifter. The experimental result of $\Delta\phi/\Delta T$ is different from the calculation. The discrepancy is most likely caused by temperature gradients between the inside of the TWRR and the measuring points. Finally, we calculated the ratio $\Delta x/\Delta T$ from $\Delta\phi/\Delta x$ and $\Delta\phi/\Delta T$. It is necessary to know the ratio $\Delta x/\Delta T$ to keep the multiplication factor maximum with the phase shifter for the design point 20% duty operation.

Using this information, we could accelerate the electron beam with a macropulse average beam current of 100 mA, a pulse width of 1 ms and a repetition rate of 35 pps up to 7 MeV. At these operation parameters we encountered problems typical of those found in high-power, high-duty electron linacs. The most significant problem is heat-up of the beam ducts caused by a beam halo. At present, we are working to improve beam quality so as to reduce the beam halo by optimizing the injector part. After this we will increase the average beam current and then achieve a beam power of 200 kW.

Acknowledgements

The authors would like to thank Dr. Y. Torizuka and Dr. I. Sato for their encouragement.

The authors also wish to thank KEK injection group for giving useful advice.

References

[1] S. Toyama et al., Transmutation of long-lived fission product (^{137}Cs, ^{90}Sr) by a reactor–accelerator system, in: Proceedings of the second International Symposium on Advanced Nuclear Energy Research, Japan, 1990, p. 387.

[2] R. Shersby Harvie, R.B. Mullet, L.B. Mullett, Proc. Phys. Soc. (London) B 62 (1949) 270.

[3] Y.L. Wang et al., J. Nucl. Sci. Technol. 30 (12) (1993) 1261.

[4] Y.L. Wang et al., Accelerator structure of PNC high power quasi-CW electron linac, in: Proceedings of the 11th Symposium on Accelerator Science and Technology, Japan, 1997, p. 233.

[5] M. Nakamura, Japanese J. Appl. Phys. 7 (3) (1968) 257.